Iranian Journal of
Mathematical Chemistry

IJMC

DOI: 10.22052/IJMC.2025.255411.1998
Vol. 16, No. 4, 2025, pp. 355-372
Research Paper

The Symmetric Division Eccentric Index of Two Infinite Classes of Fullerenes

Ivan Dler Ali[1], Herish Omer Abdullah[1] and Modjtaba Ghorbani[2*]

[1]Department of Mathematics, Salahaddin University-Erbil, Kurdistan, Iraq

[2]Department of Mathematics, Faculty of Science, Shahid Rajaee Teacher Training University, Tehran, 16785-163, I. R. Iran

Keywords:

Symmetric division eccentric index,
Eccentricity,
Fullerene graphs

AMS Subject Classification (2020):

05C07; 92E10

Article History:

Received: 4 April 2025
Accepted: 3 October 2025

Abstract

A fullerene graph is a 3-connected, planar cubic graph where each face is either pentagonal or hexagonal. This paper investigates the symmetric division eccentric index (SDE) of fullerenes, particularly focusing on two infinite classes F_{10n} and F_{12n}. We establish several bounds for fullerene graphs. We also explore the automorphism group actions on the vertices and edges of these fullerene graphs, establishing a relation between edge orbits and their eccentricities. General formulas for calculating SDE-indices are derived for F_{10n}, when $n \geq 8$ and F_{12n}, when $n \geq 10$. Furthermore, we present a new approach to compute the SDE-index and then implement the method to obtain general formulas for the SDE-index of the given classes of fullerenes.

1 Introduction

Complex systems analysis has gained prominence across physics, chemistry, and biology, demanding tools beyond traditional methods. Graph theory offers a powerful framework, representing these systems as networks where nodes signify entities and edges represent their interactions. This paper introduces the symmetric division eccentric (SDE) index, a novel graph invariant that extends the symmetric division degree index by using vertex eccentricities instead of degrees. We analyze the SDE-index for two infinite families of fullerene graphs, F_{10n} ($n \geq 8$) and F_{12n} ($n \geq 10$). This work contributes to understanding graph structural properties and suggests further research into the SDE-index and its applications.

Fullerene graphs are mathematical paradigms of fullerene molecules. Conventionally, a fullerene

*Corresponding author
E-mail addresses: evan.ali1@su.edu.krd (I. Dler Ali), herish_omer69@yahoo.com (H. O. Abdullah), mghorbani@sru.ac.ir (M. Ghorbani)
Academic Editor: Abbas Saadatmandi

graph is a three-connected plane cubic graph in which every face is a pentagon or a hexagon. These structures depict a unique class of carbon-cage molecules, where carbon atoms are arranged in a nearly spherical layout. These structures exhibit remarkable chemical and physical properties, making them of significant interest in fields such as nanotechnology, materials science, and medicinal chemistry. Many authors have studied various indices of different families of fullerenes [1, 2].

Icosahedral arrangements of carbon atoms have also been observed since the 1980s, collectively known as fullerenes. The most prominent icosahedral fullerene is the buckyball C_{60} [3], which in mathematical nomenclature is called a truncated icosahedron and has the shape of a football. All these cages share the property that carbon atoms each have three bonds to other carbon atoms of roughly the same length and angle, namely, fullerene cages are three-connected, see [4]. Although the fullerene molecules were theoretically predicted and discussed [3], it was nevertheless a surprise for the largest part of the scientific community when Kroto et al. published a paper announcing their experimental discovery. Yet, the basic geometry and symmetry behind such structures was known at least since 1937 when Goldberg discussed a class of polyhedra, now often called Goldberg polyhedra, consisting only pentagonal and hexagonal faces [5].

Fullerenes, such as C_{60} (Buckminsterfullerene), are known for their high symmetry and stability. They consist of 12 pentagonal and $\left(\frac{n}{2} - 10\right)$ hexagonal faces, where n is the number of carbon atoms and $n \neq 22$ is a natural number equal to or greater than 20.

The study of fullerenes extends beyond their chemical properties to their topological characteristics, which can be analyzed using various graph theoretical indices. The symmetric division eccentric (SDE) index is one such measure that captures the distribution of eccentricities among the vertices of a graph.

Throughout this paper, our terminology and notations, in general, will be standard; for other definitions, we refer the reader to texts on Graph Theory, such as [6–9].

2 Main results

In theoretical chemistry, topological indices are major tools for computing the properties of molecular compounds. Throughout this paper, we consider only simple connected graphs. The vertex and edge sets of a graph G are denoted by $V(G)$ and $E(G)$, respectively. The distance between two vertices u and v in $V(G)$, denoted by $d(u,v)$, is defined as the length of the shortest path connecting u and v.

The symmetric division eccentric index is a newly defined graph invariant given by the following formula [10–12]

$$SDE(G) = \sum_{uv \in E} \frac{\varepsilon^2(u) + \varepsilon^2(v)}{\varepsilon(u)\varepsilon(v)},$$

and $\varepsilon(u)$ denotes the eccentricity of vertex u.

In [13, 14], the general form of the SDD, known as the generalized symmetric division degree is defined by replacing the degree of vertices with a function f of vertex properties, denoted by $GSDD$ as

$$GSDD(G) = \sum_{uv \in E} \frac{f(u)}{f(v)} + \frac{f(v)}{f(u)},$$

where $f(u)$ and $f(v)$ denote the values of function f at vertices u and v, respectively.

Following, the SDD-index and putting $f(u) = \varepsilon(u)$ and $f(v) = \varepsilon(v)$, for every edge $e = uv$, in generalized form of SDD-index, the symmetric division eccentric index is defined as follows:

$$SDE(G) = \sum_{uv \in E(G)} \left(\frac{\varepsilon(u)}{\varepsilon(v)} + \frac{\varepsilon(v)}{\varepsilon(u)} \right),$$

where $\varepsilon(u)$ denotes the eccentricity of vertex u, see [15].
For the edge $e = uv \in E(G)$, we define the eccentricity of the edge e, denoted by $\varepsilon(e)$, as the ordered pair $\varepsilon(e) = [\varepsilon(u), \varepsilon(v)]$, where $\|\varepsilon(e)\| = \varepsilon(u)\varepsilon(v)$.
In following, for shorting, the eccentricity of a vertex u is also denoted by ε_u.

Lemma 2.1. *([11]). Suppose G is a graph, and $A_1, A_2, \ldots, A_t$ are the edge-orbits of $\mathrm{Aut}(G)$ under its action on $E(G)$. Let $e_i = u_i v_i \in A_i$ $(1 \leq i \leq t)$. Then*

$$SDE(G) = \sum_{j=1}^{t} |A_j| \left(\frac{\varepsilon_{u_j}}{\varepsilon_{v_j}} + \frac{\varepsilon_{v_j}}{\varepsilon_{u_j}} \right).$$

In particular, if G is edge-transitive, then

$$SDE(G) = 2m \quad or \quad SDE(G) = \left(\frac{a^2 + b^2}{ab} \right) m,$$

for some a and b.

3 The symmetric division eccentric index of two classes of fullerenes

A bijection σ on the vertex set of graph G is named an automorphism of the graph if it preserves the edge set. In other words, σ is an automorphism if $e = uv$ is an edge, then $\sigma(e) = \sigma(u)\sigma(v)$ is an edge of E. Let $Aut(G) = \{\alpha : V \to V,\ \alpha\ is\, bijection\}$, then $Aut(G)$ under the composition of mappings forms a group. $Aut(G)$ acts transitively on V if for any vertices u and v in V there is $\alpha \in Aut(G)$ such that $\alpha(u) = v$.

The goal of this section is to compute the symmetric division eccentric index of two infinite classes of fullerenes, namely F_{10n} and F_{12n}, where $n \geq 8$ and $n \geq 10$, respectively. We begin by considering the infinite class of fullerenes with exactly $10n$ vertices and $15n$ edges, depicted in Figure 1. The symmetric division eccentric index of F_{10n} for $2 \leq n \leq 7$ is presented in Table 11. For $n \geq 8$, a general formula for the symmetric division eccentric index of F_{10n} will be derived in this section.

Next, we present a new approach for calculating the symmetric division eccentric index of graphs. We then implement this method to obtain general formulas for the sde-index of two infinite classes of fullerenes.
For an edge $e = uv$ of a graph G, the sde of an edge e is denoted by $sde(e)$. Hence,

$$sde(e) = \frac{\varepsilon(u)}{\varepsilon(v)} + \frac{\varepsilon(v)}{\varepsilon(u)},$$

and then

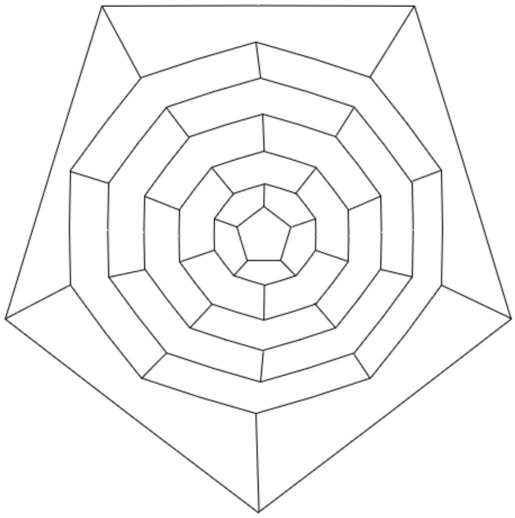

Figure 1: The molecular graph of the fullerene graph F_{10n}, where $n = 6$.

$$SDE(G) = \sum_{e \in E(G)} sde(e).$$

We define a relation $\mathcal{R}$ on the set of edges of a graph G as follows: for $e, f \in E(G)$, we say that e is related to f, denoted by $e\mathcal{R}f$, if and only if $sde(e) = sde(f)$. It is not difficult to verify that $\mathcal{R}$ is an equivalence relation on $E(G)$. Consequently, $\mathcal{R}$ induces a partition of $E(G)$ into r disjoint equivalence classes $\mathcal{E}_1, \mathcal{E}_2, \ldots, \mathcal{E}_r$. For $e \in E(G)$, the equivalence class $[e]_{\mathcal{R}} = \{f \in E(G) \mid e\mathcal{R}f\}$ is denoted by $\mathcal{E}_i$, for $i = 1, 2, \ldots, r$. Therefore, we have $E(G) = \bigcup_{i=1}^{r} \mathcal{E}_i$.

Fact 1. For any two edges e and f in the same edge orbit $\mathbb{E}$ of a graph G, we have $sde(e) = sde(f)$. However, the converse does not hold. This means that if $sde(e) = sde(f)$, it does not necessarily follow that e and f belong to the same edge orbit $\mathbb{E}$.

Fact 2. Let G be a self-centered graph. Then the eccentricities of all vertices of G are the same and G has only one $\mathcal{R}$-class. This implies that $sde(e) = 2$ for all edges e of G. Therefore,

$$SDE(G) = \sum_{e \in E(G)} sde(e) = 2|E|.$$

Example 3.1. The Petersen graph P_e is a graph with 10 vertices, 15 edges, and 3-regular. Since the radius and diameter of the Petersen graph P_e are equal, then the graph is self-centered. Therefor, by using Fact 2 we get

$$SDE(P_e) = 2|E| = 2(15) = 30.$$

Fact 3. If G is an edge-transitive or a bi-centered graph, then the contribution of all edges is the same, and we have only one edge orbit. Consequently, $sde(e) = sde(f)$ for any e and f of G. This implies that

$$SDE(G) = \sum_{e \in E(G)} sde(e) = |E|\, sde(e),$$

for an arbitrary edge e.

Example 3.2. The Gray graph, denoted by G_r, is the smallest trivalent semi-symmetric graph. It is 3-regular and edge-transitive but not vertex-transitive [16]. It is a bipartite graph with 54 vertices and 81 edges. Then,

$$SDE(G_r) = \sum_{e \in E(G_r)} \mathrm{sde}(e) = |E| \cdot \mathrm{sde}(e),$$

for an arbitrary edge e of G_r.
Since $\varepsilon(u) = 6$ for any vertex u in G_r, the value of $\mathrm{sde}(e)$ for any edge $e \in E(G_r)$ is

$$sde(e) = 2.$$

Therefore, the symmetric division eccentric index for the Gray graph is given by

$$SDE(G_r) = 2 \times 81 = 162.$$

Fact 4. If G is a vertex-transitive graph then for any edge $e = uv$ in $E(G)$, we have

$$\varepsilon(u) = \varepsilon(v),$$

and thus

$$SDE(G) = 2|E(G)|.$$

Lemma 3.3. *Let $\mathcal{E}_1, \mathcal{E}_2, \ldots, \mathcal{E}_r$ be the classes of a graph G under the relation $\mathcal{R}$ on the set of edges $E(G)$, and let $e_i = u_i v_i \in \mathcal{E}_i$, for $1 \leq i \leq r$. Then*

$$SDE(G) = \sum_{i=1}^{r} \sum_{e_i \in \mathcal{E}_i} |\mathcal{E}_i| \left(\frac{\varepsilon(u_i)^2 + \varepsilon(v_i)^2}{\|\varepsilon(e_i)\|} \right). \tag{1}$$

Proof. Let $\mathcal{E}_i$ for $i = 1, 2, \ldots, r$ be the equivalence classes of the graph G under the relation $\mathcal{R}$ on the set $E(G)$. Since, for any two edges e and f in the same $\mathcal{R}$-classes of G, we have $sde(e) = sde(f)$, it follows that $E(G) = \bigcup_{i=1}^{r} \mathcal{E}_i$. Therefore, the result follows. ∎

Now, given that the fullerene F_n, with order n and size m, is a 3-regular graph, it follows immediately that $2m = 3n$. Therefore

$$\begin{aligned} SDE(F_n) &= \sum_{uv \in E(F_n)} \frac{\varepsilon(u)^2 + \varepsilon(v)^2}{\varepsilon(u)\varepsilon(v)} = \sum_{uv \in E(F_n)} \left(\frac{(\varepsilon(u) - \varepsilon(v))^2 + 2\varepsilon(u)\varepsilon(v)}{\varepsilon(u)\varepsilon(v)} \right) \\ &= 3n + \sum_{uv \in E(F_n)} \frac{(\varepsilon(u) - \varepsilon(v))^2}{\|\varepsilon(e)\|}. \end{aligned} \tag{2}$$

By combining Equations (1), (2) and utilizing the fact that $|\varepsilon(u) - \varepsilon(v)| \leq 1$ for any two adjacent vertices u and v in $V(F_n)$, we derive the following useful formula.

Corollary 3.4. *For the fullerene graph F_n on n vertices, we have*

$$SDE(F_n) = 3n + \sum_{\substack{uv \in E(F_n) \\ \varepsilon(u) \neq \varepsilon(v)}} \frac{1}{\|\varepsilon(e)\|}.$$

Based on the findings outlined above, we arrive at the following definition.

Definition 3.5. The generalized second eccentric Zagreb index of the molecular graph G, $EM_2^{\alpha}(G)$, is a new topological index defined as

$$EM_2^{\alpha}(G) = \sum_{uv\in E(G)} (\varepsilon(u)\varepsilon(v))^{\alpha}, \quad \text{for } \alpha \in \mathbb{R}.$$

Thus, we can conclude that

$$SDE(F_n) = 3n + EM_2^{-1}(F_n).$$

We know that for any graph G, $r \leq \varepsilon(u) \leq d$, where r and d are the radius and diameter of G, respectively.
Now, for the fullerene F_n on n vertices and for any edge $e = uv$, we have

$$\frac{1}{\varepsilon(u)\varepsilon(v)} \geq \frac{1}{d^2} \quad \text{and} \quad \frac{1}{\varepsilon(u)\varepsilon(v)} \leq \frac{1}{r^2}.$$

Therefore

$$SDE(F_n) \geq 3n + \sum_{\substack{uv\in E(G)\\ \varepsilon(u)\neq\varepsilon(v)}} \frac{1}{d^2} = 3n + \frac{t}{d^2},$$

and

$$SDE(F_n) \leq 3n + \sum_{\substack{uv\in E(G)\\ \varepsilon(u)\neq\varepsilon(v)}} \frac{1}{r^2} = 3n + \frac{t}{r^2},$$

in which t is the number of edges $e = uv$ satisfying $\varepsilon(u) \neq \varepsilon(v)$.
Hence, we arrive at the following result.

Corollary 3.6. *For the fullerene graph F_n on n vertices, we have*

$$3n + \frac{t}{d^2} \leq SDE(F_n) \leq 3n + \frac{t}{r^2},$$

in which t is the number of edges $e = uv$ of F_n satisfying $\varepsilon(u) \neq \varepsilon(v)$.

In [17], Ghorbani and Rahmani demonstrated that the fullerene graph F_{10n} as depicted in Figure 2, for even n (odd n), has n orbits under the action of the automorphism group on the set of vertices, and they computed the n members of each orbit. They also showed that F_{10n}, for even n (odd n), has $n+1$ orbits under the action of the automorphism group on the set of edges. It is known that the automorphism group $\mathrm{Aut}(G)$ acting on the vertex set $V(G)$ is closely related to its action on the edge set $E(G)$. Following the approach in [17], we obtain the $n+1$ orbits of F_{10n}, for even and odd n under the action of the automorphism group on the set of edges. The $n+1$ orbits of F_{10n} as depicted in Figure 3, for even n, are shown in Table 1. The first $\frac{n}{2}$ orbits correspond to edges within layers, while the remaining $\frac{n}{2}+1$ orbits consist of the vertical edges.

The $n+1$ orbits of F_{10n}, for odd n under the action of the automorphism group on the set of edges, are given in Table 2. The first $\frac{n+1}{2}$ orbits correspond to edges within layers while the remaining $\frac{n+1}{2}$ orbits consist of the vertical edges.

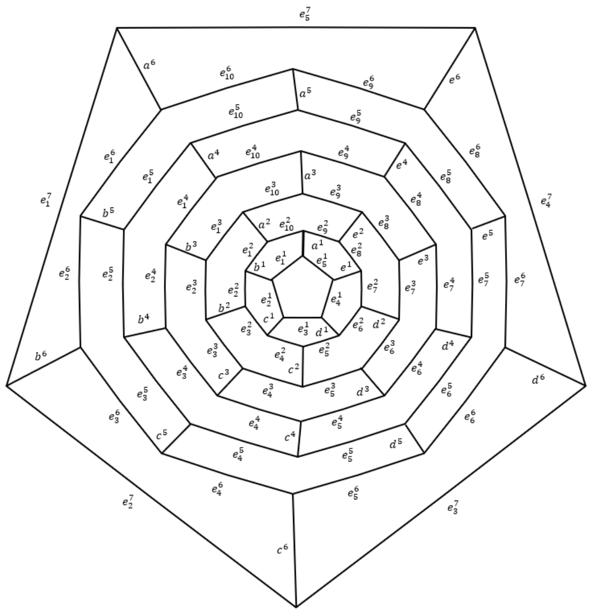

Figure 2: The planar graph of F_{10n}, where n is even ($n = 6$).

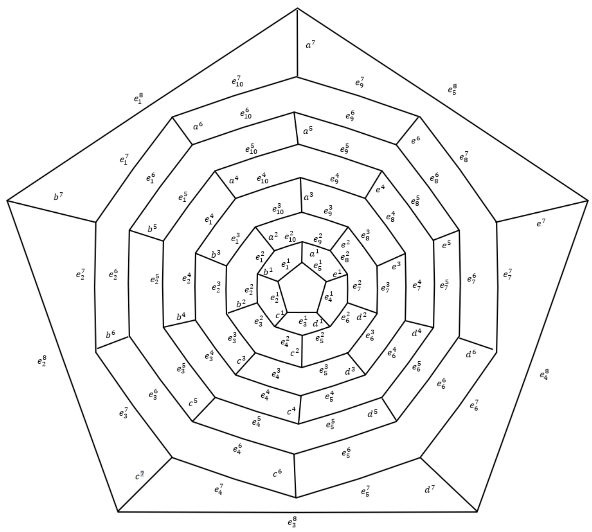

Figure 3: The planar graph F_{10n}, where n is odd ($n = 7$).

Table 1: Members of the edge orbits of F_{10n}, for even n.

Orbit	Edge orbit members	Number
$\mathbb{E}_1$	$e_1^1, e_2^1, e_3^1, e_4^1, e_5^1, e_1^{(n+1)}, e_2^{(n+1)}, e_3^{(n+1)}, e_4^{(n+1)}, e_5^{(n+1)}$	10
$\mathbb{E}_2$	$e_1^2, e_2^2, e_3^2, \ldots, e_{10}^2, e_1^n, e_2^n, e_3^n, \ldots, e_{10}^n$	20
$\mathbb{E}_3$	$e_1^3, e_2^3, e_3^3, \ldots, e_{10}^3, e_1^{(n-1)}, e_2^{(n-1)}, e_3^{(n-1)}, \ldots, e_{10}^{(n-1)}$	20
$\vdots$	$\vdots$	$\vdots$
$\mathbb{E}_{n/2}$	$e_1^{(n/2+1)}, e_2^{(n/2+1)}, e_3^{(n/2+1)}, \ldots, e_{10}^{(n/2+1)}$	10
$\mathbb{E}_{n/2+1}$	$a^1, b^1, c^1, d^1, e^1, a^n, b^n, c^n, d^n, e^n$	10
$\mathbb{E}_{n/2+2}$	$a^2, b^2, c^2, d^2, e^2, a^{(n-1)}, b^{(n-1)}, c^{(n-1)}, d^{(n-1)}, e^{(n-1)}$	10
$\mathbb{E}_{n/2+3}$	$a^3, b^3, c^3, d^3, e^3, a^{(n-2)}, b^{(n-2)}, c^{(n-2)}, d^{(n-2)}, e^{(n-2)}$	10
$\vdots$	$\vdots$	$\vdots$
$\mathbb{E}_{n+1}$	$a^{(n/2)}, b^{(n/2)}, c^{(n/2)}, d^{(n/2)}, e^{(n/2)}, a^{(n/2+1)}, b^{(n/2+1)}, c^{(n/2+1)}, d^{(n/2+1)}, e^{(n/2+1)}$	10

Table 2: Members of the edge orbits of F_{10n}, for odd n.

Orbit	Edge orbit members	Number
$\mathbb{E}_1$	$e_1^1, e_2^1, e_3^1, e_4^1, e_5^1, e_1^{(n+1)}, e_2^{(n+1)}, e_3^{(n+1)}, e_4^{(n+1)}, e_5^{(n+1)}$	10
$\mathbb{E}_2$	$e_1^2, e_2^2, e_3^2, \ldots, e_{10}^2, e_1^n, e_2^n, e_3^n, \ldots, e_{10}^n$	20
$\mathbb{E}_3$	$e_1^3, e_2^3, e_3^3, \ldots, e_{10}^3, e_1^{(n-1)}, e_2^{(n-1)}, e_3^{(n-1)}, \ldots, e_{10}^{(n-1)}$	20
$\vdots$	$\vdots$	$\vdots$
$\mathbb{E}_{(n+1)/2}$	$e_1^{(n+1)/2}, e_2^{(n+1)/2}, e_3^{(n+1)/2}, \ldots, e_{10}^{(n+1)/2}, e_1^{(n+3)/2}, e_2^{(n+3)/2}, e_3^{(n+3)/2}, \ldots, e_{10}^{(n+3)/2}$	20
$\mathbb{E}_{(n+3)/2}$	$a^1, b^1, c^1, d^1, e^1, a^n, b^n, c^n, d^n, e^n$	10
$\mathbb{E}_{(n+5)/2}$	$a^2, b^2, c^2, d^2, e^2, a^{(n-1)}, b^{(n-1)}, c^{(n-1)}, d^{(n-1)}, e^{(n-1)}$	10
$\mathbb{E}_{(n+7)/2}$	$a^3, b^3, c^3, d^3, e^3, a^{(n-2)}, b^{(n-2)}, c^{(n-2)}, d^{(n-2)}, e^{(n-2)}$	10
$\vdots$	$\vdots$	$\vdots$
$\mathbb{E}_{n+1}$	$a^{(n+1)/2}, b^{(n+1)/2}, c^{(n+1)/2}, d^{(n+1)/2}, e^{(n+1)/2}$	5

Since any two edges e and f of $E(F_{10n})$ in the same edge orbit $\mathbb{E}_i$ satisfy $sde(e) = sde(f)$, it follows that the relation $\mathcal{R}$ induces a partition of $E(F_{10n})$ into n disjoint equivalence classes $\mathcal{E}_1, \mathcal{E}_2, \ldots, \mathcal{E}_n$. It is clear that

$$E(F_{10n}) = \bigcup_{i=1}^{n} \mathcal{E}_i.$$

We classify the n classes under the relation $\mathcal{R}$ on the set of edges, and the corresponding number of elements for each class of F_{10n}, for even $n \geq 8$, are obtained and given in Table 3. The first $\frac{n}{2}$ classes correspond to edges within cycle layers, while the remaining $\frac{n}{2}$ classes consist of the vertical edges.

Table 3: Members of the edge classes of F_{10n}, for even $n \geq 8$.

Partition	$\mathcal{R}$-classes members	Number
$\mathcal{E}_1$	$e_1^1, e_2^1, e_3^1, e_4^1, e_5^1, e_1^{n+1}, e_2^{n+1}, e_3^{n+1}, e_4^{n+1}, e_5^{n+1},$ $e_1^{n/2+1}, e_2^{n/2+1}, e_3^{n/2+1}, \ldots, e_{10}^{n/2+1}$	20
$\mathcal{E}_2$	$e_1^2, e_2^2, e_3^2, \ldots, e_{10}^2, e_1^n, e_2^n, e_3^n, \ldots, e_{10}^n$	20
$\mathcal{E}_3$	$e_1^3, e_2^3, e_3^3, \ldots, e_{10}^3, e_1^{n-1}, e_2^{n-1}, e_3^{n-1}, \ldots, e_{10}^{n-1}$	20
$\vdots$	$\vdots$	$\vdots$
$\mathcal{E}_{n/2}$	$e_1^{n/2}, e_2^{n/2}, e_3^{n/2}, \ldots, e_{10}^{n/2}, e_1^{n/2+2}, e_2^{n/2+2}, \ldots, e_{10}^{n/2+2}$	20
$\mathcal{E}_{n/2+1}$	$a^1, b^1, c^1, d^1, e^1, a^n, b^n, c^n, d^n, e^n$	10
$\mathcal{E}_{n/2+2}$	$a^2, b^2, c^2, d^2, e^2, a^{n-1}, b^{n-1}, c^{n-1}, d^{n-1}, e^{n-1}$	10
$\mathcal{E}_{n/2+3}$	$a^3, b^3, c^3, d^3, e^3, a^{n-2}, b^{n-2}, c^{n-2}, d^{n-2}, e^{n-2}$	10
$\vdots$	$\vdots$	$\vdots$
$\mathcal{E}_n$	$a^{n/2}, b^{n/2}, c^{n/2}, d^{n/2}, e^{n/2}, a^{n/2+1}, b^{n/2+1}, c^{n/2+1},$ $d^{n/2+1}, e^{n/2+1}$	10

The n classes under the relation $\mathcal{R}$ on the set of edges of F_{10n}, for odd $n \geq 9$, are given in Table 4. The first $\frac{n+1}{2}$ classes correspond to edges within cycle layers, while the remaining $\frac{n-1}{2}$ classes consist of the vertical edges.

Table 4: Members of the edge classes of F_{10n}, for odd $n \geq 9$.

Partition	$\mathcal{R}$-classes members	Number
$\mathcal{E}_1$	$e_1^1, e_2^1, e_3^1, e_4^1, e_5^1, e_1^{n+1}, e_2^{n+1}, e_3^{n+1}, e_4^{n+1}, e_5^{n+1},$ $a^{(n+1)/2}, b^{(n+1)/2}, c^{(n+1)/2}, d^{(n+1)/2}, e^{(n+1)/2}$	15
$\mathcal{E}_2$	$e_1^2, e_2^2, e_3^2, \ldots, e_{10}^2, e_1^n, e_2^n, e_3^n, \ldots, e_{10}^n$	20
$\mathcal{E}_3$	$e_1^3, e_2^3, e_3^3, \ldots, e_{10}^3, e_1^{n-1}, e_2^{n-1}, e_3^{n-1}, \ldots, e_{10}^{n-1}$	20
$\vdots$	$\vdots$	$\vdots$
$\mathcal{E}_{(n+1)/2}$	$e_1^{(n+1)/2}, e_2^{(n+1)/2}, e_3^{(n+1)/2}, \ldots, e_{10}^{(n+1)/2},$ $e_1^{(n+3)/2}, e_2^{(n+3)/2}, \ldots, e_{10}^{(n+3)/2}$	20
$\mathcal{E}_{(n+3)/2}$	$a^1, b^1, c^1, d^1, e^1, a^n, b^n, c^n, d^n, e^n$	10
$\mathcal{E}_{(n+5)/2}$	$a^2, b^2, c^2, d^2, e^2, a^{n-1}, b^{n-1}, c^{n-1}, d^{n-1}, e^{n-1}$	10
$\mathcal{E}_{(n+7)/2}$	$a^3, b^3, c^3, d^3, e^3, a^{n-2}, b^{n-2}, c^{n-2}, d^{n-2}, e^{n-2}$	10
$\vdots$	$\vdots$	$\vdots$
$\mathcal{E}_n$	$a^{(n-1)/2}, b^{(n-1)/2}, c^{(n-1)/2}, d^{(n-1)/2}, e^{(n-1)/2},$ $a^{(n+3)/2}, b^{(n+3)/2}, c^{(n+3)/2}, d^{(n+3)/2}, e^{(n+3)/2}$	10

Some exceptional cases of the $\mathcal{R}$-classes of F_{10n} for $2 \leq n \leq 7$ are presented in Table 5, detailing the number of edges in each partition. Additionally, the $sde(e)$ for an arbitrary edge e in each partition is presented.

Table 5: Some exceptional cases of the edge partitions of F_{10n}, for $2 \leq n \leq 7$.

Fullerenes	# Edge Partitions	$\lvert\mathcal{E}_i\rvert$	$sde(\text{e})$ $e \in \mathcal{E}_i$
F_{20}	1	30	2
F_{30}	1	45	2
F_{40}	3	40, 10, 10	2, 2.018, 2.024
F_{50}	3	55, 10, 10	2, 2.014, 2.018
F_{60}	5	40, 20, 10, 10, 10	2, 2.011, 2.009, 2.014, 2.018
F_{70}	6	35, 20, 20, 10, 10, 10	2, 2.007, 2.011, 2.006, 2.009, 2.014

We illustrate these ideas in the following example.

Example 3.7. Consider the fullerene F_{40}, as depicted in Figure 4. It is clear that $|V(F_{40})| = 40$ and $|E(F_{40})| = 60$. The classes of F_{40} under the relation $\mathcal{R}$ on the set of edges, the number of elements of each class, and for an arbitrary edge e in each class, the corresponding eccentricities of their end vertices are given in Table 6.

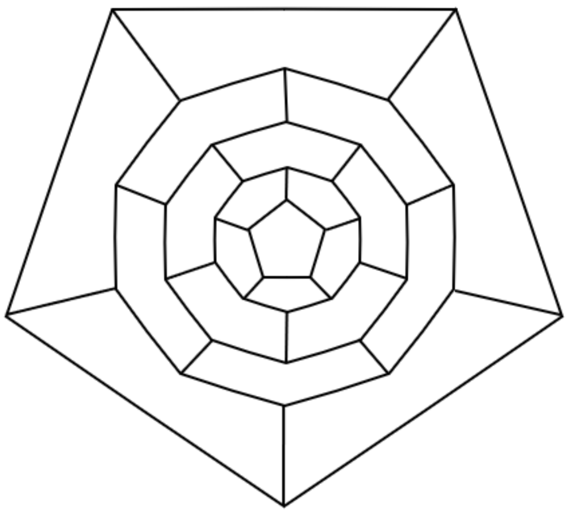

Figure 4: The planar graph of fullerene F_{10n}, where $n = 4$.

Now, by applying Corollary 3.4, we obtain

$$SDE(F_{40}) = 3(40) + \frac{10}{7.8} + \frac{10}{6.7} = 120 + 0.238095 + 0.1785714 \approx 120.41667.$$

The following result follows from the preceding discussion, Lemma 3.3 and Corollary 3.6.

Theorem 3.8. *The SDE-index of the fullerene graph F_{10n} for $n \geq 8$ is given as*

$$(a)\ SDE(F_{10n}) = 30n + 10\left(\frac{1}{n} - \frac{2}{2n-1}\right) + 10\sum_{i=1}^{n/2} f_i,$$

Table 6: Edge partitions of the fullerene F_{40}.

Partition	Class members	Number	$\varepsilon(u),\varepsilon(v)$
$\mathcal{E}_1$	$e_1^1, e_2^1, e_3^1, e_4^1, e_5^1, e_1^5, e_2^5, e_3^5, e_4^5, e_5^5,$ $e_1^2, e_2^2, e_3^2, \ldots, e_{10}^2, e_1^4, e_2^4, e_3^4, \ldots, e_{10}^4,$ $e_1^3, e_2^3, e_3^3, \ldots, e_{10}^3$	40	$8,8$
$\mathcal{E}_2$	$a^1, b^1, c^1, d^1, e^1, a^4, b^4, c^4, d^4, e^4$	10	$7,8$
$\mathcal{E}_3$	$a^2, b^2, c^2, d^2, e^2, a^3, b^3, c^3, d^3, e^3$	10	$6,7$

where

$$f_i = \left[\frac{1}{2(n-i)} + \frac{1}{2(n-i)+1} - \frac{2}{2(n-i)+2}\right],$$

and n is even.

$$(b) SDE(F_{10n}) = 30n + 10 \sum_{i=1}^{(n-1)/2} f_i,$$

where

$$f_i = \left[\frac{2}{2(n-i)-1} - \frac{1}{2(n-i)} - \frac{1}{2(n-i)+1}\right],$$

and n is odd.

Proof. Let $\mathcal{E}_1, \mathcal{E}_2, \ldots, \mathcal{E}_n$ be all $\mathcal{R}$-classes of the fullerene F_{10n}, $n \geq 8$, given in Tables 3 and 4 under the relation $\mathcal{R}$ on the set of edges $E(F_n)$, and $e_i = u_i v_i \in \mathcal{E}_i$, satisfying $\varepsilon(u_i) \neq \varepsilon(v_i)$, for $1 \leq i \leq n$. Then we have

$$SDE(F_{10n}) = 30n + \sum_{i=1}^{n} \sum_{\substack{u_i v_i \in \mathcal{E}_i \\ \varepsilon(u_i) \neq \varepsilon(v_i)}} \frac{|\mathcal{E}_i|}{\|\varepsilon(e_i)\|}. \quad (3)$$

a) If n is even, then we classify the edges of F_{10n} into two main types:
1) Ring edges (see Table 7): These consist of edges in the i-th layer, where $1 \leq i \leq n+1$. Each layer forms a cycle, and the vertices within each cycle are connected via ring edges.
2) Vertical edges(see Table 8): These include the vertical edges that connect a vertex u in the i-th layer to a vertex v in the $(i+1)$-th layer, where $1 \leq i \leq n-1$. The vertical edges connect vertices between adjacent layers, maintaining the structure of the fullerene graph. The eccentricities of vertices u and v for both types of edges (ring and vertical) are provided in the Tables 7 and 8.

Due to the symmetry of the fullerene graph F_{10n} and for even n, we observe that the eccentricities of the ring edges in the first layer are identical to those corresponding edges in the $(n+1)$th layer, the eccentricities of the ring edges in the second layer are identical to those corresponding edges in the n-th layer, and this pattern continues, with the eccentricities of the ring edges in the $\frac{n}{2}$th layer being identical to those corresponding edges in the $\left(\frac{n}{2}+2\right)$th layer. The same symmetry holds for the vertical edges. Now, using Tables 3, 7 and 8 and

Table 7: Ring edges of the fullerene F_{10n}, with even $n \geq 8$.

i	$\varepsilon(u)$	$\varepsilon(v)$	# Edges
1	$2n-1$	$2n-1$	5
$2 \leq i \leq \frac{n}{2}$	$2(n-i)+2$	$2(n-i)+1$	$5(n-2)$
$i = \frac{n}{2}+1$	n	n	n
$\frac{n}{2}+2 \leq i \leq n$	$2(i-2)+2$	$2(i-2)+1$	$5(n-2)$
$n+1$	$2n-1$	$2n-1$	5

Table 8: Vertical edges of the fullerene F_{10n}, with even $n \geq 8$.

i	$\varepsilon(u)$	$\varepsilon(v)$	# Edges
$1 \leq i \leq \frac{n}{2}$	$2(n-i)+1$	$2(n-i)$	$\frac{5}{2}n$
$\frac{n}{2}+1 \leq i \leq n$	$2(i-1)+1$	$2(i-1)$	$\frac{5}{2}n$

Corollary 3.6, we arrive at

$$\begin{aligned} SDE(F_{10n}) =& 30n + \sum_{i=1}^{n} \sum_{\substack{u_i v_i \in \mathcal{E}_i \\ \varepsilon(u_i) \neq \varepsilon(v_i)}} \frac{|\mathcal{E}_i|}{\|\varepsilon(e_i)\|} \\ =& 30n + 20 \sum_{i=2}^{n/2} \frac{1}{[2(n-i)+2][2(n-i)+1]} \\ &+ 10 \sum_{i=1}^{n/2} \frac{1}{[2(n-i)+1][2(n-i)]}. \end{aligned}$$

Finally, by simplifying the above formula, we get $SDE(F_{10n})$ as given in the statement of the theorem part (a).

b) If n is odd, then again we classify the edges of F_{10n} into two main types:
1)Ring edges (see Table 9), which consist of edges in the i-th layer, for $1 \leq i \leq n+1$.
2) Vertical edges (see Table 10), which include the vertical edges connecting a vertex u in the i-th layer to vertex v in the $(i+1)$-th layer, for $1 \leq i \leq n-1$. The eccentricities of u and v for both types are given in the Tables 9 and 10.

Table 9: Ring edges of the fullerene F_{10n}, with odd $n \geq 9$.

i	$\varepsilon(u)$	$\varepsilon(v)$	# Edges
1	$2n-1$	$2n-1$	5
$2 \leq i \leq \frac{n+1}{2}$	$2(n-i)+2$	$2(n-i)+1$	$5(n-1)$
$\frac{n+3}{2} \leq i \leq n$	$2(i-2)+2$	$2(i-2)+1$	$5(n-1)$
$n+1$	$2n-1$	$2n-1$	5

Similar to the last case, agian symmetry of the fullerene graph F_{10n} yields that for odd n the eccentricities of the ring edges in the first layer are identical to those corresponding edges in the $(n+1)$th layer, the eccentricities of the ring edges in the second layer are identical to those corresponding edges in the nth layer, and this pattern continues, with the eccentricities of the ring edges in the $\frac{(n+1)}{2}$th layer being identical to those corresponding edges in the $\frac{(n+3)}{2}$th

Table 10: Vertical edges of the fullerene F_{10n}, with odd $n \geq 9$.

i	$\varepsilon(u)$	$\varepsilon(v)$	# Edges
$1 \leq i \leq \frac{n-1}{2}$	$2(n-i)+1$	$2(n-i)$	$\frac{5}{2}(n-1)$
$\frac{n+1}{2}$	n	n	5
$\frac{n+3}{2} \leq i \leq n$	$2(i-1)+1$	$2(i-1)$	$\frac{5}{2}(n-1)$

layer. The same symmetry holds for the vertical edges. Now, using Tables 4, 9 and 10, and Corollary 3.6, we arrive at

$$\begin{aligned} SDE(F_{10n}) =& 30n + \sum_{i=1}^{n} \sum_{\substack{u_i v_i \in \mathcal{E}_i \\ \varepsilon(u_i) \neq \varepsilon(v_i)}} \frac{|\mathcal{E}_i|}{\|\varepsilon(e_i)\|} \\ =& 30n + 20 \sum_{i=2}^{(n+1)/2} \frac{1}{[2(n-i)+2][2(n-i)+1]} \\ &+ 10 \sum_{i=1}^{(n-1)/2} \frac{1}{[2(n-i)+1][2(n-i)]}. \end{aligned}$$

Finally, by simplifying the above formula, we get $SDE(F_{10n})$ as given in the statement of the theorem part (b). Some exceptional cases of Theorem 3.8 are presented in the Table 11.

Table 11: Some exceptional cases of Theorem 3.8

Fullerenes	Some exceptional symmetric division eccentric index for $2 \leq n \leq 7$
F_{20}	60
F_{30}	90
F_{40}	120.4166667
F_{50}	150.3174603
F_{60}	180.6305916
F_{70}	210.6676379

■

Consider now an infinite class of fullerenes with exactly $12n$ vertices and $18n$ edges, depicted in Figure 5. By applying similar techniques and methods as in the proof of Theorem 3.8, we obtain the symmetric division eccentric index of the fullerene F_{12n}, as given below.

Theorem 3.9. *The SDE-index of the fullerene graph F_{12n} for $n \geq 10$ is given by*

$$(a)\ SDE(F_{12n}) = 36n + 12\left(\frac{1}{n} - \frac{2}{2n-1}\right) + 12\sum_{i=1}^{n/2} f_i,$$

where

$$f_i = \left[\frac{1}{2(n-i)} + \frac{1}{2(n-i)+1} - \frac{2}{2(n-i)+2}\right],$$

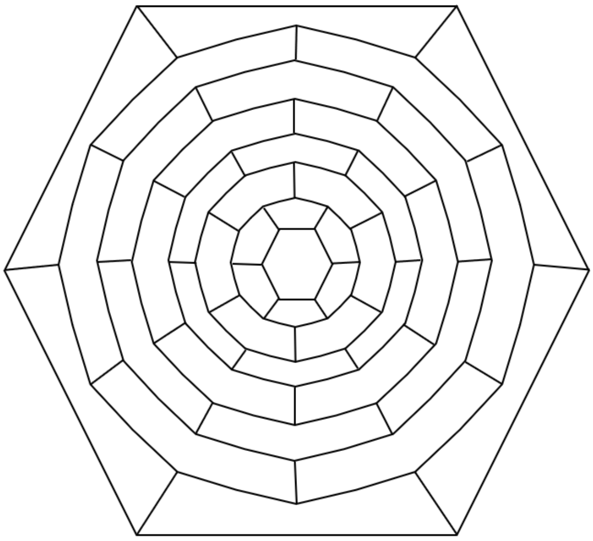

Figure 5: The planar graph of fullerene F_{12n} where $n = 7$.

and n is even.

$$(b)\ SDE(F_{12n}) = 36n + 12 \sum_{i=1}^{(n-1)/2} f_i,$$

where

$$f_i = \left[\frac{2}{2(n-i)-1} - \frac{1}{2(n-i)} - \frac{1}{2(n-i)+1}\right],$$

and n is odd.

Proof. The proof is straightforward. The exeptional cases are given in Table 12. ■

Table 12: Some exceptional symmetric division eccentric index for $2 \leq n \leq 9$.

Fullerenes	Some exceptional symmetric division eccentric index for $2 \leq n \leq 9$
F_{24}	72
F_{36}	108
F_{48}	144.2142857
F_{60}	180.3
F_{72}	216.4090909
F_{84}	252.5011655
F_{96}	288.6901765
F_{108}	324.7009608

Theorem 3.10. *For a fullerene graph F_{10n} with $n \geq 8$ vertices, the SDE-index satisfies the following inequalities:*

$$\frac{15n(8n^2 - 12n + 5)}{2(2n-1)(n-1)} \leq SDE(F_{10n}) \leq \frac{15(2n^2 + 2n + 1)}{n+1}.$$

Proof. By [18, Theorem 3] , the radius and diameter of F_{10n} are given by n and $2n-2$, respectively. Using the fact that $r \le \varepsilon(u) \le d$, where r is the radius and d is the diameter, we obtain:

$$SDE(F_{10n}) \le \left(\frac{r}{r+1} + \frac{r+1}{r}\right) m.$$

Substituting $r = n$, we get:

$$SDE(F_{10n}) \le \left(\frac{n}{n+1} + \frac{n+1}{n}\right) m = \frac{15(2n^2+2n+1)}{n+1}.$$

On the other hand, since

$$SDE(F_{10n}) \ge \left(\frac{d}{d+1} + \frac{d+1}{d}\right) m,$$

substituting $d = 2n-2$, we get:

$$SDE(F_{10n}) \ge \left(\frac{2n-2}{2n-1} + \frac{2n-1}{2n-2}\right) m = \frac{15n(8n^2-12n+5)}{2(2n-1)(n-1)}.$$

This completes the proof. ∎

By a similar way, using [18, Theorem 2], we find that $rad(F_{12n}) = n$ and $diam(F_{12n}) = 2n-1$ and thus we conclude the following result.

Theorem 3.11. *For a fullerene F_{12n} with $n \ge 10$ vertices, the SDE-index satisfies the following inequalities:*

$$\frac{18(2n^2+2n+1)}{n+1} \le SDE(F_{12n}) \le \frac{9(8n^2-4n+1)}{2n-1}.$$

4 Conclusion

The link between the calculated SDE index and boiling points is examined in this section using regression models. Table 13 lists 30 different fullerenes, each with a unique identifier, their corresponding SDE values, and their boiling points. The SDE value and boiling points are provided in numerical form, allowing for a quantitative analysis.

The relationship between the SDE index and the boiling point of fullerenes was systematically examined using several regression models. The dataset of 30 fullerenes (Table 13) provided a reliable basis for evaluating the predictive capacity of the SDE index. Regression analyses were performed in SPSS, and the results are presented in Table 14.

The statistical outputs indicate that all regression models tested (linear, quadratic, cubic, logarithmic, and exponential) are highly significant, with P-values less than 0.05, see Figure 6. This demonstrates that the SDE index is strongly correlated with the boiling point of fullerenes. However, the strength of association, measured by the coefficient of determination (R^2), varied across models.

The quadratic and cubic models achieved the highest R^2 values (0.998), confirming their excellent ability to describe the nonlinear relationship between SDE and boiling point. The linear regression model also performed very well (R^2=0.978), suggesting that even a simple linear equation captures most of the variability in the data. The logarithmic model (R^2=0.971)

Table 13: SDE index and boiling point data for fullerenes.

No.	# F	SDE	Bp	No.	# F	SDE	Bp
1	F_{20}	60	381.6	16	F_{50}	150	753.8
2	F_{24}	72	443.5	17	F_{50}	150.43	753.8
3	F_{26}	78.2	472.4	18	F_{52}	156.32	773.6
4	F_{28}	85.2	500.1	19	F_{54}	162.46	793.0
5	F_{30}	90.6	526.8	20	F_{60}	180	849
6	F_{30}	90.333	526.4	21	F_{72}	216.67	952.9
7	F_{32}	96.14	552.6	22	F_{74}	222.71	969.2
8	F_{34}	102.1	577.5	23	F_{80}	240	1017
9	F_{36}	108.19	601.7	24	F_{100}	300.15	1296
10	F_{38}	114	625.1	25	F_{120}	360.18	1417
11	F_{40}	120	647.9	26	F_{140}	420.37	1530
12	F_{40}	120	647.9	27	F_{160}	480.39	1635
13	F_{40}	138.48	691.8	28	F_{180}	540.53	1735
14	F_{42}	126	670.1	29	F_{200}	600.52	1829
15	F_{48}	144.21	733.6	30	F_{220}	660.66	1933

Table 14: Model summary and parameter estimates.

Equation	R Square	F	Sig.	Constant	b1	b2	b3
Linear	.978	1230.972	.000	329.137	2.656		
Logarithmic	.971	949.360	.000	-2498.150	662.097		
Quadratic	.998	7381.019	.000	148.883	4.389	-.003	
Cubic	.998	4929.912	.000	130.058	4.654	-.004	9.232E-7
Exponential	.892	232.125	.000	465.867	.003		

showed slightly weaker performance, while the exponential model (R^2=0.892) was the least accurate.

Despite the superior fit of the quadratic and cubic models, the linear regression was chosen as the most appropriate model for interpretation and prediction. This preference is justified by its simplicity, reduced risk of overfitting, and ease of application in practical settings. Moreover, the small difference in predictive power between the linear and higher-order models indicates that the added complexity of polynomial equations does not yield substantial improvement.

The findings highlight a strong quantitative relationship between the SDE index and the boiling point of fullerenes. The consistency across different regression models reinforces the robustness of the SDE index as a reliable topological descriptor. In particular, the high predictive ability of the linear model underscores its value in correlating structural features of fullerenes with their physicochemical properties.

Beyond fullerenes, these results contribute to the broader understanding of how topological indices can serve as powerful descriptors for physicochemical and thermodynamic properties in diverse chemical systems. Previous studies have shown that indices such as Wiener, Zagreb, and Randić provide useful correlations in alkanes, benzenoids, and other molecular classes. The present findings extend this utility to the SDE index, suggesting its potential for application in predicting stability, reactivity, and phase behavior across a wider range of nanostructures and molecular frameworks. Consequently, the SDE index may play an important role in computational chemistry, materials science, and the rational design of novel carbon-based nanomaterials.

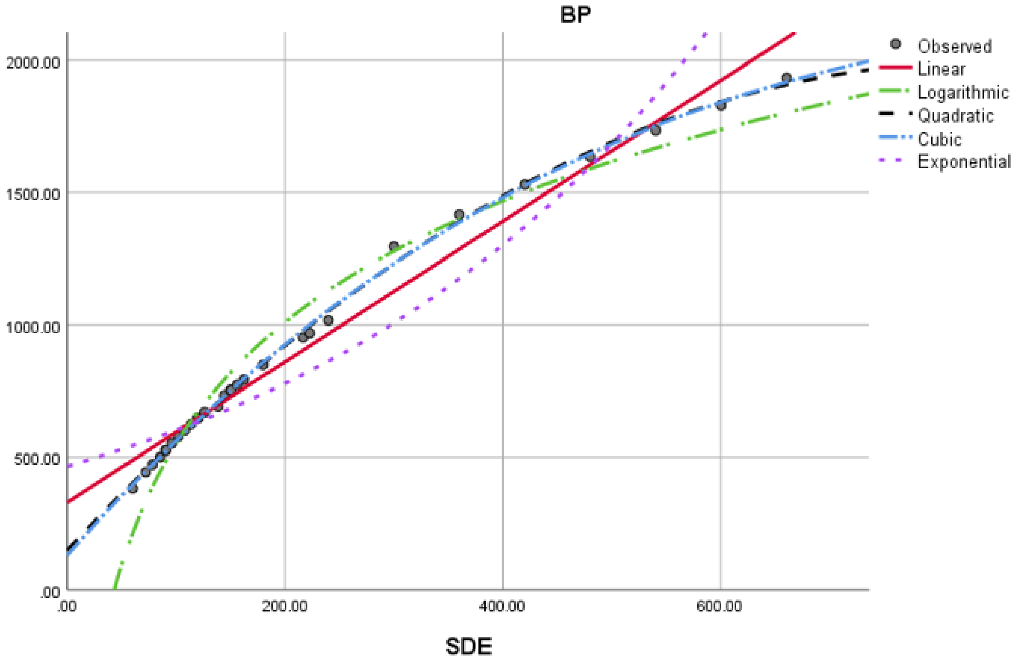

Figure 6: The scatter plot of correlation between SDE index and boiling points of fullerenes.

Conflicts of Interest. The authors declare that they have no conflicts of interest regarding the publication of this article.

Acknowledgement. The research of the third author was partially supported by Shahid Rajaee Teacher Training University under grant number 27043854/03.

References

[1] V. Andova, T. Doslić, M. Krnc, B. Lužar and R. Škrekovski, On the diameter and some related invariants of fullerene graphs, *MATCH Commun. Math. Comput. Chem.* **68** (2012) #109.

[2] M. Ghorbani, R. Alidehi-Ravandi and M. Dehmer, Fullerenes via their counting polynomials, *Appl. Math. Comput.* **466** (2024) #128431, https://doi.org/10.1016/j.amc.2023.128431.

[3] H. W. Kroto, J. R. Heath, S. C. O'Brien, R. F. Curl and R. E. Smalley, C_{60}-Buckminsterfullerene, *Nature* **318** (1985) 162–163.

[4] P. P. Dechant, J. Wardman, T. Keef and R. Twarock, Viruses and fullerenes-symmetry as a common thread?, *Acta Crystallogr., Sect. A: Found. Adv.* **70** (2014) 162–167, https://doi.org/10.1107/S2053273313034220.

[5] M. Goldberg, A class of multi-symmetric polyhedra, *Tohoku Math. J.* **43** (1937) 104–108.

[6] M. Songhori, Eccentric connectivity index of fullerene graphs, *J. Disc. Math. Appl.* **2** (2012) 21–27.

[7] R. Sharafdini, M. Azadimotlagh, V. Hashemi and F. Parsanejad, On eccentric adjacency index of graphs and trees, *Math. Interdisc. Res.* **8** (2023) 1–17, https://doi.org/10.22052/MIR.2023.246384.1391.

[8] M. Azari, On eccentricity version of Zagreb coincides, *Math. Interdisc. Res.* **6** (2021) 107–120, https://doi.org/10.22052/MIR.2021.240325.1247.

[9] M. Itagi Huilgol and P. H. Shobha, Steiner k-eccentric connectivity index: a novel steiner distance-based index, *Iranian J. Math. Chem.* **15** (2024) 175–187, https://doi.org/10.22052/IJMC.2024.253927.1790.

[10] M. Ghorbani and R. Alidehi-Ravandi, Exploring the SDE index: a novel approach using eccentricity in graph analysis, *J. Appl. Math. Comput.* **70** (2024) 947–967, https://doi.org/10.1007/s12190-023-01980-7.

[11] M. Ghorbani, R. Alidehi-Ravandi, I. Dler Ali and O. Abdullah Herish, Exploring the symmetric division eccentric index of fullerenes: a topological approach, *Fuller. Nanotub. Car. N.* **33** (2025) 693–698, https://doi.org/10.1080/1536383X.2024.2447351.

[12] M. Ghorbani, R. Alidehi-Ravandi, N. Amraei and Z. Raza, On the largest eigenvalue of extended eccentric matrix, *Chaos Solitons Fractals* **185** (2024) #115074, https://doi.org/10.1016/j.chaos.2024.115074.

[13] N. Amraei, A generalized version of symmetric division degree index, *J. Disc. Math. Appl.* **7** (2022) 119–126, https://doi.org/10.22061/JDMA.2023.2072.

[14] N. Amraei, A survey on symmetric division degree index, *J. Disc. Math. Appl.* **7** (2022) 237–251, https://doi.org/10.22061/JDMA.2023.9656.1048.

[15] N. Amraei and A. Zaeembashi, Edge deletion and symmetric division degree index of graphs, *J. Disc. Math. Appl.* **8** (2023) 137–145, https://doi.org/10.22061/JDMA.2023.9811.1053.

[16] I. Z. Bouwer, On edge but not vertex transitive regular graphs, *J. Combin. Theory, B* **12** (1972) 32–40, https://doi.org/10.1016/0095-8956(72)90030-5.

[17] M. Ghorbani and S. Rahmani, The Mostar index of fullerenes in terms of automorphism group, *Facta Univ. Ser. Math. Inform.* **35** (2020) 151–165, https://doi.org/10.22190/FUMI2001151G.

[18] A. R. Ashrafi and M. Ghorbani, Distance matrix and diameter of two infinite family of fullerenes, *Optoelectron. Adv. Mater. – Rapid Commun.* **3** (2009) 596–599.